Channel allocation in elastic optical networks using traveling salesman problem algorithms

(article starts on next page)

Channel Allocation in Elastic Optical Networks Using Traveling Salesman Problem Algorithms

Chayan Bhar, Erik Agrell, *Fellow, IEEE*, Kamran Keykhosravi, Magnus Karlsson, *Fellow, OSA; Senior Member, IEEE*, Peter A. Andrekson, *Fellow, OSA; Fellow, IEEE*

Abstract—Elastic optical networks have been proposed to support high data-rates in metro and core networks. However, frequency allocation of the channels (i.e., channel ordering) in such networks is a challenging problem. This requires arrangement of the optical channels within the frequency grid with the objective of ensuring a minimum signal-to-noise ratio (SNR). An optimal arrangement results in the highest SNR margin for the entire network. However, searching for the optimal arrangement requires an exhaustive search through all possible arrangements (permutations) of the channels. The search space increases exponentially with the number of channels. This discourages an algorithm employing exhaustive search for the optimal frequency allocation. We utilize the Gaussian noise (GN) model to formulate the frequency allocation (channel ordering) problem as a variant of the traveling salesman problem (TSP) using graph theory. Thereafter, we utilize graph-theoretic tools for TSP from the existing literature to solve the channel ordering problem. Performance figures obtained for the proposed scheme is illustrated to be marginally inferior to the optimal search (through all possible permutations) and outperforms any random allocation scheme. Moreover, the proposed scheme is implementable for a scenario with a large number of channels. In comparison, exhaustive search with the GN model and split-step Fourier method simulations are shown to be feasible for a small number of channels only. It is also illustrated that the SNR reduces with an increase in bandwidth when the frequency separation is high.

Index Terms—graph-theoretic resource allocation, frequency allocation using TSP, SNR maximization, elastic optical networks.

I. INTRODUCTION

Optical metro and core networks face an ever increasing bandwidth demand due to the increasing end-user demands. Moreover, there have been proposals for utilizing the optical networks for front-hauling and back-hauling future wireless access networks [1]. Therefore, the bandwidth demand from future optical networks is deemed to increase exponentially with the introduction of bandwidth-heavy 5G applications. Optical networks utilizing coherent channels allow the network designer to support high data-rates. Moreover, network operators are expected to dynamically allocate resources within the networks as a function of the traffic demand [2].

Chayan Bhar, Erik Agrell and Kamran Keykhosravi are with the Department of Electrical Engineering, Chalmers University of Technology, SE-41296 Gothenburg, Sweden. (e-mail: chayan@chalmers.se)

M. Karlsson and Peter A. Andrekson are with the Department of Microtechnology and Nanoscience, Chalmers University of Technology, SE-41296 Gothenburg, Sweden.

The paradigm of elastic optical networks (EONs) has been proposed [3]–[6] for facilitating high data-rates while simultaneously improving spectrum utilization within the core and metro networks. The degrees of freedom for the network designer in an EON are the power spectral density (PSD) [7], spectrum allocation, and modulation format of the channels [8]. This necessitates implementation of routing and spectrum allocation schemes [9], [10]. Optical channels with different modulations and bandwidths can also share a single link in EONs. This results in complicated and significant non-linear interference (NLI) between the channels sharing the fiber link. Routing, modulation level, and spectrum allocation algorithms have been proposed in the literature to address these issues [3], [8], [10].

Additionally, it is essential to ensure a quality of transmission (QoT) to all channels in an EON. Existing literature on QoT for EONs can be found in two directions: (i) QoT aware resource allocation, and (ii) QoT estimation for the designed network. Research contributions of the first type assume that each channel in the network adheres to an signal-to-noise ratio (SNR) threshold. Thereafter, spectrum allocation, PSD, modulation format, and routing is decided for the channels as a function of the traffic demand [7], [8], [11]–[13], whereas research contributions of the second type observe the effect of provisioning (activating) new light paths on the QoT of all channels [14].

In metro and core networks, it is desirable for the network providers to ensure an SNR margin that is satisfied by all channels. Much of the existing literature on spectrum allocation is dedicated towards performing channel allocation from the perspective of maximizing the data-rates, given that the SNR margin that should be ensured is known. For example, the authors of [7], [15], [16] proposed schemes to maximize the bandwidth of channels and derive the modulation format by assuming that a minimum SNR margin is satisfied at all channels, whereas the authors of [12] proposed a scheme to reduce the spectral usage using an mixed integer linear programming formulation, with SNR being a parameter for the optimization. Therefore, the minimum SNR margin required is an input parameter for optimization problems in the existing literature. However, current literature does not answer the question: what SNR margin can be ensured to all channels with the knowledge of channel PSDs, channel bandwidths and frequency separation. This problem of channel ordering affects the SNR values of all channels and is referred to as the channel ordering problem (COP) in this paper.

We approach the problem of maximizing the SNR margin

that can be ensured to all channels in the network with the knowledge of the respective PSDs and bandwidths. We use the GN model to present SNR of a particular channel as a function of the NLI resulting from adjacent channels. Thereafter, we utilize the characteristics of the GN model to formulate the COP as a graph-theoretic problem. Furthermore, we draw a solution from the existing literature for traveling salesman problems (TSPs) to solve the resource allocation problem. This allows us to obtain an SNR margin by maximizing the minimum SNR experienced by any channel in the network and the associated channel order.

Graph-theoretic tools have been used in the literature for receiver scheduling in visible light communications [17], [18]. The techniques used in these papers utilize conflict graphs to solve a graph coloring problem. Such approaches are used to prevent collisions on a particular domain. *However, to the best of our knowledge, graph-theoretic tools have not been previously used for resource allocation in EONs.*

The rest of this paper is organized as follows. In the next section we model the COP as a graph-theoretic problem using some realistic assumptions. In Section III we describe the algorithm to solve the COP. This is followed by illustrating the performance of the proposed algorithm in Section IV. Finally, Section V concludes the paper.

II. MODELING THE CHANNEL ORDERING PROBLEM AS THE TRAVELING SALESMAN PROBLEM

In this section we first state the assumptions that are used throughout the paper. Thereafter, we use the GN model derived in [19], [15] to express SNR as a function of the channel ordering. This motivates the formulation of the COP as a graph-theoretic problem.

A. Problem statement

In the considered network (metro or core), n coherent channels $\mathcal{C} = \{C_1, \ldots, C_n\}$ should be transmitted over a WDM link with a fixed channel spacing F in the frequency grid. This is a valid and realistic assumption, because the network providers plan to keep dense WDM transmission on the installed equipment while introducing network efficiency and flexibility through transceiver replacement [11]. Moreover, the currently deployed multiplexers and demultiplexers prevent variable channel spacing in the frequency grid although the channel bandwidths can be variable within the fixed channel spacing (F can be adjusted to suit different network scenarios). The network is assumed to traverse through N_s spans. For each channel C_i, the power $p(C_i)$ and bandwidth $\Delta(C_i)$ are given by the corresponding traffic demands and can vary among the channels. The PSD is $G(C_i) = p(C_i)/\Delta(C_i)$.

Due to the interference between channels, the SNR experienced by each channel will depend on the channel ordering. The network designer has the task of solving the COP problem, which means finding a suitable arrangement of the n channels in the frequency grid. We represent a channel arrangement with $\boldsymbol{P} = [P_1, \ldots, P_n]$, which is an arbitrary permutation of $[C_1, \ldots, C_n]$. Here P_1 is the channel with lowest frequency and P_n the highest. The amplifier noise

figure is assumed to be the same for all channels. In this work, the objective is to find $\boldsymbol{P}$ which maximizes the SNR margin of the considered network.

B. Utilization of the GN model

The model parameters are summarized in Table I. The GN model presented in [19], [15] derives the PSD of the NLI in one span of a particular coherent channel P_i of $\boldsymbol{P}$ as a function of the PSD of its neighboring channels j, their bandwidths, and frequency spacing $|i - j|F$ as

$$G_{\text{sp}}^{\text{NLI}}(P_i) = \frac{3\gamma^2 G(P_i)}{2\pi\alpha\,|\beta_2|} \left[G^2(P_i)\sinh^{-1}\left|\frac{\pi^2\,(\Delta(P_i))^2\,\beta_2}{\alpha}\right| \right.$$
$$\left. + \sum_{\substack{j=1 \\ j \neq i}}^{n} G^2(P_j)\ln\left(\frac{|i-j|F + \Delta(P_j)/2}{|i-j|F - \Delta(P_j)/2}\right) \right]. \quad (1)$$

The first term in (1) is the self-channel interference (SCI) term while the second term results from cross-channel interference (XCI).

The overall NLI experienced by P_i is accumulated over N_s spans and is given by $G^{\text{NLI}}(P_i) = G_{\text{sp}}^{\text{NLI}}(P_i)N_s$. The SNR of P_i is

$$SNR(P_i) = \frac{G(P_i)}{G^{\text{ASE}}(P_i) + G^{\text{NLI}}(P_i)} \quad (2)$$

where assuming ν is the frequency of light, n_{sp} is the spontaneous emission factor, L is the length of a span, and h is the Planck constant

$$G^{\text{ASE}}(P_i) = \left(e^{\alpha L} - 1\right)h\nu n_{\text{sp}}N_s \quad (3)$$

is the PSD of the amplified spontaneous emission (ASE) noise affecting P_i. The amplifier gain is assumed to be equal to the signal attenuation in one span. Therefore, the noise figure of the amplifier can be calculated according to [20, (7.2.15)] as,

$$F_{\text{n}} = 2n_{\text{sp}} \quad (4)$$

We also assume that a transceiver penalty of t_{p} is present due to signal generation and reception. This results in reduction of the SNR in (2) by t_{p}. However, t_{p} is independent of F, $p(C_i)$, and $\Delta(C_i)$ and does not affect the COP. Therefore, we solve the COP using (2).

It can be deduced from (1) and (2) that when $p(P_i)$, $\Delta(P_i)$ and F are known, $SNR(P_i)$ depends on $p(P_{i+1})$, $\Delta(P_{i+1})$, $p(P_{i-1})$, $\Delta(P_{i-1})$, and so on. Therefore, the SNR figures of all channels depend on their ordering (arrangement) in $\boldsymbol{P}$, resulting in the COP. We define the minimum SNR in an arrangement $\boldsymbol{P}$ as

$$S\check{N}R = \min_i SNR(P_i). \quad (5)$$

In the next section we discuss the formulation of the COP as a max-min problem to solve for the maximum $S\check{N}R$ using graph-theoretic tools.

Symbol	Description	Numerical value
γ	Non-linear coefficient of the fiber	$1.32 \cdot 10^{-3}$ (Wm)$^{-1}$
α	Power attenuation factor	0.22 dB/km
ν	Frequency of light	193.55 THz
h	Planck constant	$6.63 \cdot 10^{-34}$ Js
n_{sp}	Spontaneous emission factor of the amplifier	1.58
t_{p}	Transceiver penalty due to signal generation and reception	2.5 dB
β_2	Group velocity dispersion coefficient	-21.7 ps^2/km
L	Length of a span	80 km
N_{s}	Number of spans present in the considered network	5
$\Delta(P_i)$	Bandwidth of the channel P_i	
F	Frequency spacing in the wavelength division multiplexing (WDM) grid	
$G_{\mathrm{sp}}^{\mathrm{NLI}}(P_i)$	PSD of NLI encountered in one span by i^{th} channel of $\boldsymbol{P}$	
$G(P_i)$	PSD of the ith channel in a particular arrangement $\boldsymbol{P}$	
$NSR(P_i)$	Noise-to-signal ratio experienced by P_i	

TABLE I: Symbols used for the GN model
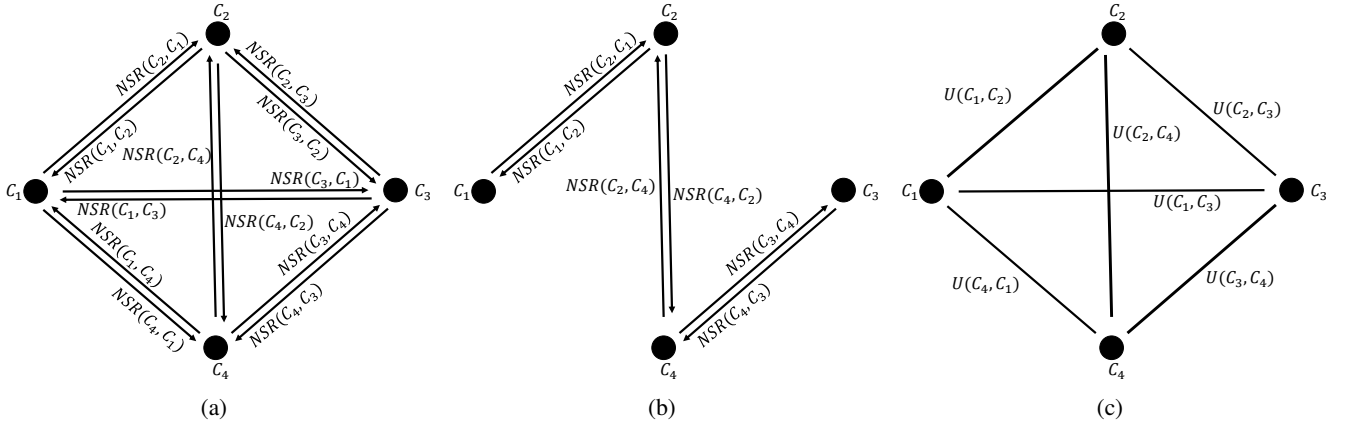
Fig. 1: Graph-theoretic formulation of the COP for an example network with four channels. (a) A directed graph $\vec{\zeta}$ based on (6). (b) A Hamiltonian path, corresponding to a certain channel arrangement $\boldsymbol{P}$. (c) An undirected graph $\bar{G}$ based on (9).

C. Problem translation into a graph

In this section we discuss the formulation of the COP targeting an arrangement $\boldsymbol{P}$, which approximately achieves the maximum $S\check{N}R$ for all channels. We work with the noise-to-signal ratio (NSR) figure which is $NSR(P_i) = 1/SNR(P_i)$. This is because the XCI terms add linearly in (1). *We assume that the cross-channel interference results only from the adjacent channels in the frequency grid, i.e., in the arrangement $\boldsymbol{P}$ of channels, P_i is affected by P_{i+1} and P_{i-1} only.* This assumption, which will be validated in Section IV-E, will enable the COP to be solved using TSP heuristics in the following.

With this assumption, using (1)–(2), the NSR of P_i is

$$NSR(P_i) = NSR(P_i, P_{i+1}) + NSR(P_i, P_{i-1}) \qquad (6)$$

where

$$
NSR(P_i, P_j) = \frac{3\gamma^2 N_{\mathrm{s}}}{2\pi\alpha|\beta_2|} \left[\frac{G(P_i)^2}{2} \sinh^{-1} \left| \frac{\pi^2\beta_2\left(\Delta(P_i)\right)^2}{\alpha} \right| \right.
$$
$$
\left. + G(P_j)^2 \ln\left(\frac{F + \Delta(P_j)/2}{F - \Delta(P_j)/2} \right) \right]
$$
$$
+ \frac{\left(e^{\alpha L} - 1\right) h\nu n_{\mathrm{sp}} N_{\mathrm{s}}}{2G(P_i)} \qquad (7)
$$

for $j = i+1$ and $i-1$. For channels P_1 and P_n, which have only one adjacent channel, we set $G(P_0) = G(P_{n+1}) = 0$ in (7).

Moreover, the problem of finding $S\check{N}R$ in (5) translates to the problem of finding the maximum NSR

$$\hat{NSR} = \max_i NSR(P_i). \qquad (8)$$

An optimal arrangement, denoted by $\hat{\boldsymbol{P}}$, is one for which $\hat{NSR}$ in (8) is minimal among all possible arrangements $\boldsymbol{P}$.

We construct a weighted directed graph $\vec{\zeta}$, such that each channel $C_i \in \mathcal{C}$ corresponds to a vertex. The edge between two vertices C_i and C_j has a weight $NSR(C_i, C_j)$, obtained by setting $P_i = C_i$ and $P_j = C_j$ in (7). Fig. 1(a) shows the graph corresponding to an example network with four channels, $\mathcal{C} = \{C_1, \dots, C_4\}$.

In a potential arrangement $\boldsymbol{P}$, any vertex can be followed by any other vertex. Therefore, $\vec{\zeta}$ so formed is a complete digraph.

The objective of the COP is to find an arrangement $\boldsymbol{P}$ connecting all the vertices, such that each vertex occurs only once in $\boldsymbol{P}$. *This corresponds to finding a Hamiltonian path $\boldsymbol{P}$ such that $\hat{NSR}$ in (8) is minimized over all possible Hamiltonian paths $\boldsymbol{P}$ in $\vec{\zeta}$.* Fig. 1(b) exemplifies one such path.

Apart from exhaustive search, which is too complex for large networks, no algorithm is known to find the optimal Hamiltonian path in the sense of (6)–(8). To reduce the complexity, we apply two further approximations. First, we define new edge weights

$$U(C_i, C_j) = \max\{NSR(C_i, C_j), NSR(C_j, C_i)\}, \quad (9)$$

which yields the undirected graph $\bar{G}$ in Fig. 1(c). Therefore, $NSR(P_i) \leq U(P_i, P_{i+1}) + U(P_i, P_{i-1})$, where both terms $U(P_i, P_{i-1})$ and $U(P_i, P_{i+1})$ are upper bounded by $\max_i U(P_i, P_{i+1})$. Moreover, $NSR(P_1) \leq U(P_1, P_2)$ and $NSR(P_n) \leq U(P_{n-1}, P_n)$. Thus, we can define a new objective function as

$$\hat{U} = 2 \max_i U(P_i, P_{(i \bmod n)+1}), \quad (10)$$

where the modulo operation converts the problem from a Hamiltonian path to a Hamiltonian cycle. We denote an arrangement for which $\hat{U}$ in (10) is minimal among all possible arrangements $\boldsymbol{P}$, with $\tilde{\boldsymbol{P}}$. From (6) and (8), we conclude that $\hat{NSR} \leq 2 \max_i NSR(P_i, P_{i\pm1})$, and from (9)–(10) that $\hat{U} \geq 2 \max_i NSR(P_i, P_{i\pm1})$. Hence $\hat{U} \geq \hat{NSR}$.

III. Solving the Traveling Salesman Problem

The objective (10) corresponds to finding a Hamiltonian cycle $\tilde{\boldsymbol{P}}$ in $\bar{G}$ such that the weight of the maximum weighted edge in $\tilde{\boldsymbol{P}}$ is minimized. This statement is the objective of a bottleneck traveling salesman problem (BTSP) algorithm [21], U_{th} being the bottleneck. In $\bar{G}$, we implement the BTSP which finds a Hamiltonian cycle $\tilde{\boldsymbol{P}}$ connecting all vertices of $\bar{G}$ such that (10) is minimized. Therefore, we specify an initial starting vertex for finding the Hamiltonian cycle and disregard the last vertex of the cycle to derive the desired $\tilde{\boldsymbol{P}}$. We refer to our proposed scheme as channel ordering using the bottleneck traveling salesman problem (COBTSP).

The BTSP algorithm implemented in this work is adapted from [22]. An algorithm for solving the BTSP consists of three steps as discussed in [22]: (i) finding an approximate upper and lower bound, (ii) translation of the edge weights, and (iii) implementation of a TSP solver. The TSP corresponds to finding the shortest Hamiltonian cycle (sum of edge weight in the chosen path) starting at a particular vertex. We next discuss these steps in brief.

1) 2-Max bound (2MB): The 2MB [23], [24] is a lower bound on the optimal value of the objective function given by (10). This bound is calculated as follows. For each channel $C_i \in \mathcal{C}$ we find the second minimum value of the weights of all edges incident on C_i, counting multiplicities (i.e., if the smallest edge weight is not unique, the second smallest edge weight is the same as the smallest edge weight). If this value for C_i is $\xi(C_i)$, then the 2MB bound is $LB = \max_i \xi(C_i)$.

Upper bound: An upper bound (UB) can be derived by using a heuristic BTSP algorithm, such as the *nearest neighbor* algorithm discussed in [21], to find any sub-optimal cycle $\boldsymbol{P}$. The value of $\hat{U}$ in (10) for this cycle gives an upper bound on the corresponding value for $\tilde{\boldsymbol{P}}$.

2) Edge weight translation: Let $\alpha_1 < \alpha_2 < \cdots < \alpha_k$ be a sorted list of all distinct edge weights $U(C_i, C_j)$ such that $LB \leq U(C_i, C_j) \leq UB$. Hence $\alpha_1 = LB$ and $\alpha_k = UB$. Let $b_l = (n^{l-1}-1)/(n-1)$ for $l = 1, \ldots, k+1$. The edge weights $U(C_i, C_j)$ are translated to $d(C_i, C_j)$ ($\in \boldsymbol{D}$) according to [22, p. 700] as

$$d(C_i, C_j) = \begin{cases} 0, & \text{if } U(C_i, C_j) < \alpha_1 \\ b_l, & \text{if } U(C_i, C_j) = \alpha_l, \ l = 1, \ldots, k \\ b_{k+1}, & \text{if } U(C_i, C_j) > \alpha_k \end{cases} \quad (11)$$

3) Utilizing a TSP solver: The BTSP is solved by implementing a TSP solver based on the so-called 2-opt algorithm [25], [26], [27] on the edge weights $d(C_i, C_j)$ as described in [22].

IV. Results and Discussion

In this section, we evaluate SNR performance of the proposed COBTSP scheme $\tilde{\boldsymbol{P}}$. The GN model for the network has been implemented in MATLAB. Moreover, exhaustive search using the split-step Fourier method (SSFM) has also been implemented in MATLAB by transmitting 10,000 symbols per WDM channel. Both the GN model and SSFM simulations use the same values of the parameters (first nine parameters in Table I). The simulations have been performed on a computer with Intel i7 3.6 GHz CPU and 32 GB RAM. For the simulations, we consider a WDM link with 5 spans, with each span being 80 km in length. The WDM grid spacing F is one of $\{50 \text{ GHz}, 100 \text{ GHz}, 200 \text{ GHz}\}$. Moreover, the channel bandwidth is assumed to be independent of the network load. The noise figure of the amplifier is calculated to be 3.16 dB by substituting the value of n_{sp} from Table I in (4), whereas t_{p} is considered to be 2.5 dB, assuming a sufficiently high duty cycle [28].

The simulation assumes Nyquist pulse shaping, so that the baud-rate is equal to the channel bandwidth. The values of the other parameters for the GN model are taken from Table I. The results are compared by considering two scenarios: (i) the number of channels, channel bandwidth, and frequency spacing are fixed, and the average channel power is varied, and (ii) the number of channels is varied with each channel power varying within a particular range. The results illustrated in this section (except Fig. 4) are obtained by averaging over 500 realizations. To study the average performance over a wide variety of transmission conditions, the channel powers for each realization were selected randomly and independently, uniformly distributed (in linear scale, not dB) within given limits, that are specified later. Finally, the averaged $\check{SNR}$ over 500 realizations is reported for each $\bar{p}$ or n. We also benchmark the performance of COBTSP $\tilde{\boldsymbol{P}}$ with an optimal channel ordering scheme $\hat{\boldsymbol{P}}$, which is only feasible when the network operates with a small number of channels (≤ 8). The performance comparison is done in terms of the SNR margin $\check{SNR}$, which in Section IV-A and IV-B is computed using the two leading XCI terms in (1) (i.e., the inverse of $\hat{NSR}$ in (8)), and in Section IV-E using additional XCI terms.
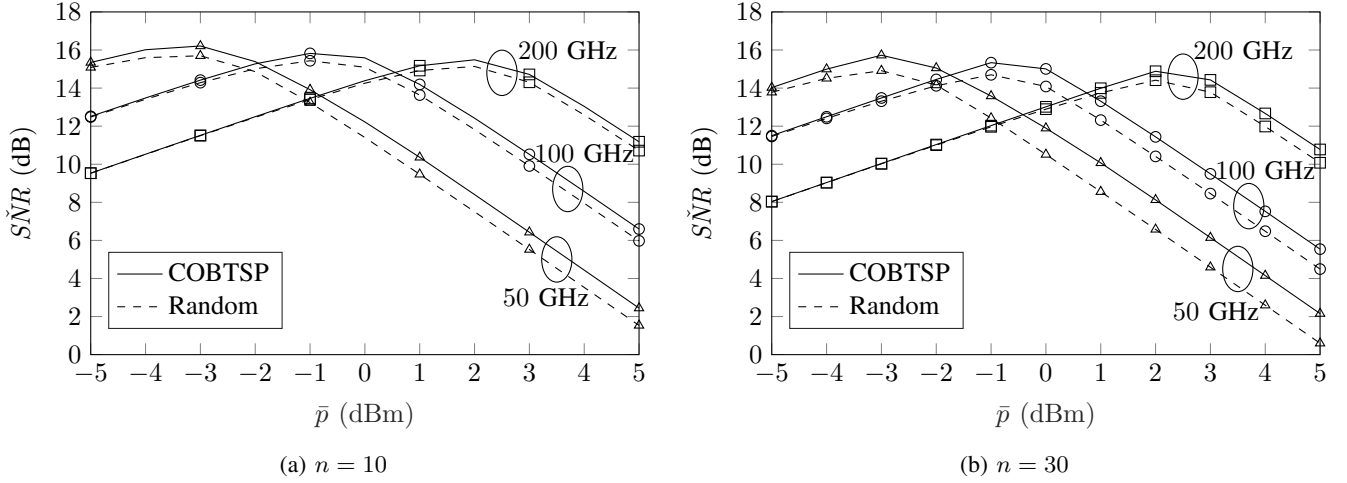
(a) $n = 10$

(b) $n = 30$

Fig. 2: Comparison of $S\check{N}R$ for scenarios with $n = 10$ and 30 channels, and $F = \Delta(P_i)$, $p(P_i) \in [\bar{p} - 5 \text{ dB}, \bar{p} + 5 \text{ dB}]$, $\forall P_i \in \mathcal{C}$.

A. SNR margin as a function of average power

For the comparisons performed in this subsection, we vary the average power $\bar{p}$ (dBm) $= \sum_{i=1}^{n} p(C_i)/n$ of the coherent channels. The individual channel powers are assumed to be uniformly distributed in linear scale within a range of ± 5 dB of the average channel power. The bandwidth of all channels is assumed to be same as F, and $S\check{N}R$ is observed for $n = 10$ and 30. The simulation results are illustrated in Fig. 2.

We make three observations from Fig. 2:

(i) The peak $S\check{N}R$ shifts to a higher $\bar{p}$ on increasing F.
(ii) A gain of about 1 dB is obtained with COBTSP at high $\bar{p}$ and (or) small F over a random allocation scheme. The gain increases with n.
(iii) The gain in $S\check{N}R$ reduces with $\bar{p}$ or increase in F.

The XCI reduces with an increase in F. This contributes to good SNR at higher average power, resulting in the first observation. Fig. 2 also motivates the necessity to choose an optimal power for the channels depending on the selected F to achieve the best SNR. The peaky nature of the plots in Fig. 2 results from the dependence of SNR on channel powers in the GN-model [19], [15].

The second observation highlights the importance of the COP and the improvement in performance due to COBTSP particularly when n is high, i.e., the network employs many channels. Fig. 2 also illustrates the effect of the average channel power on $S\check{N}R$. It is observed that on increasing $\bar{p}$ or reducing F, the difference between $S\check{N}R$ plots obtained from random allocation and COBTSP reduces. This is attributed to an increase in the nonlinear noise component with a decrease in F or due to the presence of channels having higher optical powers, resulting in the third observation. A similar observation can be made on increasing the power variance across $\bar{p}$, in which case the peak of $S\check{N}R$ will also reduce, while there will be higher a gain in $S\check{N}R$ due to COBTSP. This is discussed later with reference to Fig. 5.

B. SNR margin as a function of the number of channels

In this subsection, we compare $S\check{N}R$ for a scenario in which the power varies uniformly between -5 dBm and 5 dBm. The results are averaged over multiple realizations of channel powers as in Fig. 2. The bandwidths $\Delta(P_i)$ are 60% and 100% of F. The performance figures are illustrated in Fig. 3, which leads us to four observations.

(i) For $F = 50$ GHz and 100 GHz, $S\check{N}R$ increases with $\Delta(P_i)$.
(ii) For $F = 200$ GHz, $S\check{N}R$ reduces with an increase in $\Delta(P_i)$.
(iii) A performance gain of ≈ 1 dB is observed for COBTSP compared with the random allocation scheme.
(iv) The $S\check{N}R$ of COBTSP is close to that obtained from the optimal scheme using an exhaustive search through all possible permutations.

The first observation is related to the fact that the XCI contribution reduces with an increase in F, which results in a subsequent improvement of $S\check{N}R$. However, when F is relatively high, e.g., 200 GHz, the XCI increases with $\Delta(P_i)$, when F is kept constant. Therefore, for $\Delta(P_i) = F = 200$ GHz, $S\check{N}R$ is lower than for $\Delta(P_i) = F = 100$ GHz, as observed in the inset of Fig. 3b.

Moreover, increasing $\Delta(P_i)$ subsequently increases the optimal signal power $p(P_i)$. This is ascertained from the plot of the SNR performance as a function of $\Delta(P_i)/F$ in Fig. 4, where a scenario with three channels having equal bandwidth and power $p(P_1) = p(P_2) = p(P_3) \in \{-5, 5\}$ dBm is considered. Here $F \in \{50 \text{ GHz}, 100 \text{ GHz}, 200 \text{ GHz}\}$, while SNR variation of the middle channel is observed as a function of $\Delta(P_i)/F$. The adjacent-channel assumption of Section II-C is also considered for Fig. 4. It is observed from Fig. 4 that $S\check{N}R$ increases with $\Delta(P_i)$ for $\bar{p} = 5$ dBm and reduces with $\Delta(P_i)$ for $\bar{p} = -5$ dBm. Moreover, for $F = \Delta(P_i) = 200$ GHz, $S\check{N}R$ saturates at a higher value (17 dB) for $\bar{p} = 5$ dBm compared to that for $\bar{p} = -5$ dBm (12 dB). This leads to the second observation from Fig. 3b
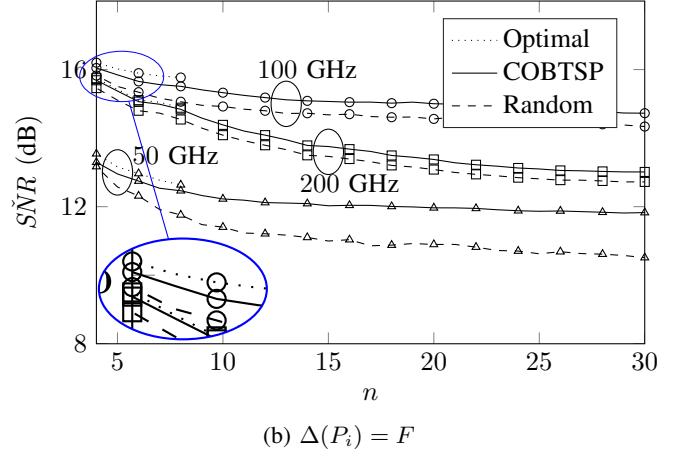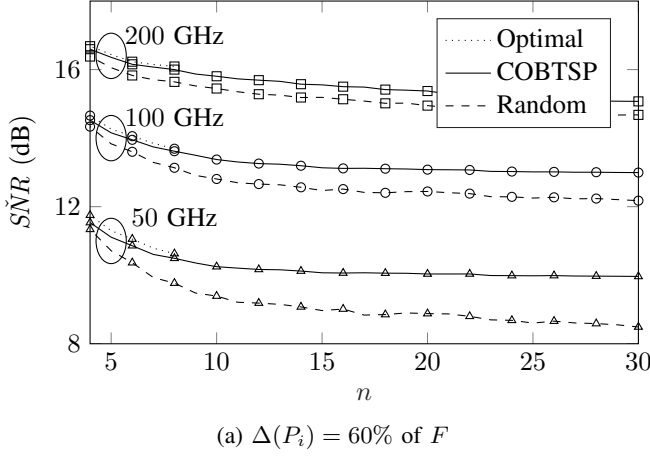
(a) $\Delta(P_i) = 60\%$ of F

(b) $\Delta(P_i) = F$

Fig. 3: Comparison of $S\check{N}R$ obtained from COBTSP, random allocation and optimal allocation (using exhaustive search) schemes as a function of n with channel power deviation of 10 dB, $p(P_i) \in \{-5 \text{ dBm}, \ldots, 5 \text{ dBm}\}$, $\forall P_i \in \mathcal{C}$, $\bar{p} = 0$ dBm.
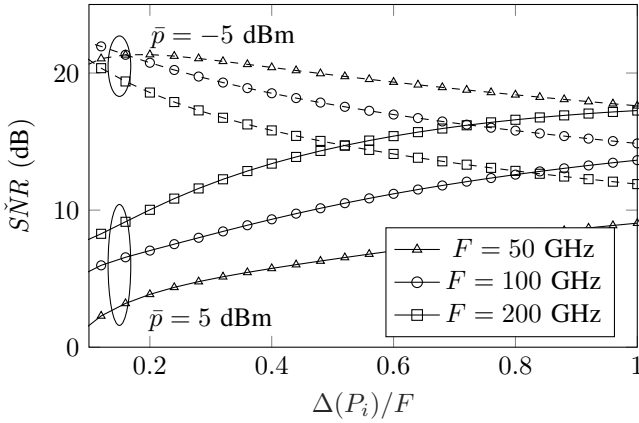

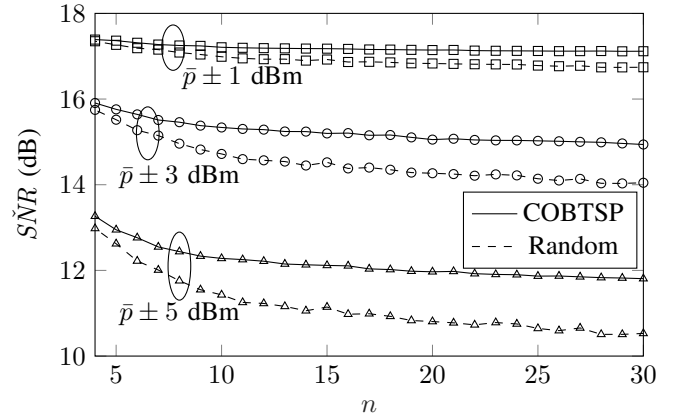Fig. 4: $S\check{N}R$ for the central channel when $n = 3$, illustrating the reason for performance flipover.

Fig. 5: Comparison of $S\check{N}R$ for $F = \Delta(P_i) = 50$ GHz, $\bar{p} = 0$ dBm and different power deviations.

and a conclusion that $\bar{p}$ can also be optimized to maximize $S\check{N}R$.

The third observation and fourth observations highlight the motivation of the COP and performance benefits of COBTSP. It is also concluded that COBTSP can be used to solve the COP even when a large number of channels are present in the network. In contrast, with reasonable computing resources it is not possible to obtain the optimal $S\check{N}R$ when more than 8 channels are considered. This is discussed in Section IV-G.

C. SNR margin as a function of the variation in channel power

In Fig. 5, we compare $S\check{N}R$ when the channel power varies within different limits, ± 1 dBm, ± 3 dBm, and ± 5 dBm. It is observed from Fig. 5 that $S\check{N}R$ is higher when the channel powers vary over a smaller range (± 1 dBm) than over a wider range (± 5 dBm). This is attributed to the low NLI when the channel powers vary over a small range. However, for a larger variation in the channel powers, the NLI significantly affects the $S\check{N}R$. In such scenarios, the difference between $S\check{N}R$ of

COBTSP and a random allocation scheme (Fig. 5) motivates the need to employ an opportunistic scheme to solve the COP.

D. Performance in an add-drop network scenario

In this subsection we consider a network scenario with $n = 30$, $\Delta(P_i) = F \in \{50 \text{ GHz}, 100 \text{ GHz}\}$ and $\bar{p} \in \{0 \text{ dBm}, -2 \text{ dBm}\}$. Channels $P_i, \ldots P_{i+k}$ ($i < n$ and $i + k \leq n$) are dropped at a node. j channels have to be added to the frequency grid at this node within the spectrum hole created by the dropped channels, with the objective of maximizing $S\check{N}R$. It is assumed that the next node is at a distance of 5 spans, with $L = 80$ km in each span. The average power of these j channels are assumed to be $\bar{p}^1 \in \{0 \text{ dBm}, 2 \text{ dBm}\}$ with bandwidth and frequency separation $\Delta(P_i^1) = F^1 \in \{50 \text{ GHz}, 100 \text{ GHz}\}$ such that $F^1 \times j = F \times k$. Assuming that only the XCI from adjacent channels is significant, Fig. 6 illustrates the minimum SNR (SNR_m^1) of channels $P_i, P_1^1, \ldots, P_j^1, P_{i+k}$ as a function of n.
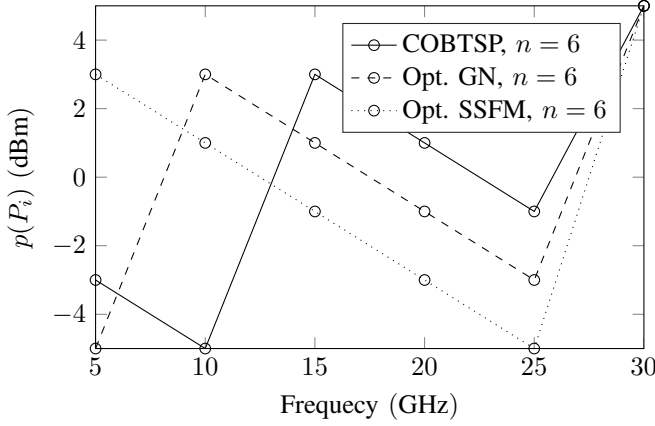
It is observed that:

Fig. 8: Optimal channel arrangement for $n = 6$ obtained from COBTSP and exhaustive search for the optimal arrangement using the GN model and SSFM (Opt. GN, Opt. SSFM) respectively.

SSFM results from mismatch of the GN model with SSFM simulations as pointed out in [30].

G. Complexity analysis of COBTSP

The 2-opt algorithm has been analyzed to have a worst case complexity of $O(n^6 \ln(n))$ [31], whereas the exhaustive search has a complexity of $O(n!)$. Solving the COP using exhaustive search with SSFM simulations takes 9.5 hours for $n = 6$. This prevents performing exhaustive search using SSFM for any higher n. Moreover, solving the COP using exhaustive search with the GN model takes approximately 9 hours for $n = 10$ with the above-mentioned computational resources. For higher n, the simulation run-times are very high, thereby preventing solution for networks with more channels. The routing and spectral allocation problems present in the literature have mixed integer linear programming formulations and are therefore NP hard [4], [32], resulting in similar exponential runtimes. In comparison, COBTSP has a computational runtime of 0.01 s for $n = 30$ with the above discussed computational resources.

V. CONCLUSIONS

In this paper we proposed a graph-theoretic solution to the COP in EONs. The proposed COBTSP scheme solves the COP in realistic networks with a large number of channels, where it is not possible to employ an optimal algorithm. In such networks, COBTSP achieves near-optimal SNRs. It is also illustrated that the peak of the SNR margin occurs at higher average channel powers, on increasing the frequency separation between the channels (Fig. 2). This gives a design criterion to the network designer. The plot of $S\check{N}R$ as a function of channel bandwidth (Fig. 4) proves that beyond a certain value of channel separation, the network designer cannot improve $S\check{N}R$ further by increasing the channel bandwidth, without adjusting the channel power. Therefore, selecting optimal channel powers can be used alongside COBTSP to ensure the best SNR margin. Moreover, $S\check{N}R$ can be made more accurate

by simultaneously considering interference from both nearby channels instead of only one channel as assumed in Section II-C. For networks that incorporate channels employing multiple modulation formats, the SNRs can be manipulated to the desired (different) values by introducing a modulation-dependent offset in (7). However, investigation in these directions is out of scope for the current work.

REFERENCES

[1] L. Velasco, A. Castro, A. Asensio, M. Ruiz, G. Liu, C. Qin, R. Proietti, and S. J. B. Yoo, "Meeting the requirements to deploy cloud RAN over optical networks," *Journal of Optical Communications and Networking*, vol. 9, no. 3, pp. B22–B32, 2017.

[2] B. Yan, Y. Zhao, X. Yu, W. Wang, Y. Wu, Y. Wang, and J. Zhang, "Tidal-traffic-aware routing and spectrum allocation in elastic optical networks," *Journal of Optical Communications and Networking*, vol. 10, no. 11, pp. 832–842, 2018.

[3] M. Klinkowski and K. Walkowiak, "Routing and spectrum assignment in spectrum sliced elastic optical path network," *IEEE Communications Letters*, vol. 15, no. 8, pp. 884–886, 2011.

[4] M. Tornatore, C. Rottondi, R. Goscien, K. Walkowiak, G. Rizzelli, and A. Morea, "On the complexity of routing and spectrum assignment in flexible-grid ring networks [Invited]," *Journal of Optical Communications and Networking*, vol. 7, no. 2, pp. A256–A267, 2015.

[5] V. Abedifar, M. Furdek, A. Muhammad, M. Eshghi, and L. Wosinska, "Routing, modulation, and spectrum assignment in programmable networks based on optical white boxes," *Journal of Optical Communications and Networking*, vol. 10, no. 9, pp. 723–735, 2018.

[6] C.-F. Hsu, Y.-C. Chang, and S.-C. Sie, "Graph-model-based dynamic routing and spectrum assignment in elastic optical networks," *Journal of Optical Communications and Networking*, vol. 8, no. 7, pp. 507–520, 2016.

[7] L. Yan, E. Agrell, H. Wymeersch, P. Johannisson, R. Di Taranto, and M. Brandt-Pearce, "Link-level resource allocation for flexible-grid nonlinear fiber-optic communication systems," *IEEE Photonics Technology Letters*, vol. 27, no. 12, pp. 1250–1253, 2015.

[8] M. Yaghubi-Namaad, A. G. Rahbar, and B. Alizadeh, "Adaptive modulation and flexible resource allocation in space-division-multiplexed elastic optical Networks," *Journal of Optical Communications and Networking*, vol. 10, no. 3, pp. 240–251, 2018.

[9] P. Afsharlar, A. Deylamsalehi, J. M. Plante, J. Zhao, and V. M. Vokkarane, "Routing and spectrum assignment with delayed allocation in elastic optical networks," *Journal of Optical Communications and Networking*, vol. 9, no. 3, pp. B101–B111, 2017.

[10] G. Z. Marković, "Routing and spectrum allocation in elastic optical networks using bee colony optimization," *Photonic Network Communications*, vol. 34, no. 3, pp. 356–374, 2017.

[11] F. P. Guiomar, R. Li, C. R. S. Fludger, A. Carena, and V. Curri, "Hybrid modulation formats enabling elastic fixed-grid optical networks," *Journal of Optical Communications and Networking*, vol. 8, no. 7, pp. A92–A100, 2016.

[12] H. Beyranvand and J. A. Salehi, "A quality-of-transmission aware dynamic routing and spectrum assignment scheme for future elastic optical networks," *Journal of Lightwave Technology*, vol. 31, no. 18, pp. 3043–3054, 2013.

[13] M. Hadi and M. R. Pakravan, "Energy-efficient resource allocation for elastic optical networks using convex optimization," *Journal of Optical Communications and Networking*, vol. 9, no. 10, pp. 889–899, 2017.

[14] I. Sartzetakis, K. Christodoulopoulos, C. P. Tsekrekos, D. Syvridis, and E. A. Varvarigos, "Quality of transmission estimation in WDM and elastic optical networks accounting for space–spectrum dependencies," *Journal of Optical Communications and Networking*, vol. 8, no. 9, pp. 676–688, 2016.

[15] L. Yan, E. Agrell, H. Wymeersch, and M. Brandt-Pearce, "Resource allocation for flexible-grid optical network with nonlinear channel model," *Journal of Optical Communications and Networking*, vol. 7, no. 11, pp. B101–B108, 2015.

[16] L. Yan, E. Agrell, M. N. Dharmaweera, and H. Wymeersch, "Joint assignment of power, routing, and spectrum in static flexible-grid networks," *Journal of Lightwave Technology*, vol. 35, no. 10, pp. 1766–1774, 2017.

[17] Y. Tao, X. Liang, J. Wang, and C. Zhao, "Scheduling for indoor visible light communication based on graph theory," *Optics Express*, vol. 23, no. 3, pp. 2737–2752, 2015.

[18] H. Liu, H. Dai, Y. Chen, and P. Xia, "Conflict graph-based downlink resource allocation and scheduling for indoor visible light communications," *Journal of the Optical Society of Korea*, vol. 20, no. 1, pp. 36–41, 2016.

[19] P. Johannisson and E. Agrell, "Modeling of nonlinear signal distortion in fiber-optical networks," *Journal of Lightwave Technology*, vol. 32, no. 23, pp. 3942–3950, 2013.

[20] G. P. Agrawal, *Fiber-optic communication systems*, 4th ed., K. Chang, Ed.   John Wiley & Sons, 2010.

[21] R. S. Garfinkel and K. C. Gilbert, "The bottleneck traveling salesman problem: Algorithms and probabilistic analysis," *Journal of the ACM*, vol. 25, no. 3, pp. 435–448, 1978.

[22] S. N. Kabadi and A. P. Punnen, "The Bottleneck TSP," in *The Traveling Salesman Problem and Its Variations*, G. Gutin and A. P. Punnen, Eds. Springer US, 2007, vol. 91, ch. 15, pp. 697–735.

[23] G. Carpaneto, M. Silvano, and P. Toth, "An algorithm for the bottleneck traveling salesman problem," *Operations Research*, vol. 32, no. 2, pp. 380–389, 1984.

[24] J. Larusic and A. P. Punnen, "The asymmetric bottleneck traveling salesman problem : Algorithms , complexity and empirical analysis," *Computers and Operation Research*, vol. 43, pp. 20–35, 2014.

[25] G. A. Croes, "A method for solving traveling salesman problems," *Operations Research*, vol. 6, no. 6, pp. 791–812, 1958.

[26] D. S. Johnson and L. A. McGeoch, "The traveling salesman problem: a case study," in *Local Search in Combinatorial Optimization*, E. Aarts and J. K. Lenstra, Eds.   Princeton University Press, Princeton, Oxford, 2003 & Sons Ltd., 2003, ch. 8, pp. 216–310.

[27] K. Helsgaun, "Effective implementation of the Lin-Kernighan traveling salesman heuristic," *European Journal of Operational Research*, vol. 126, no. 1, pp. 106–130, 2000.

[28] D. J. Geisler and J. E. Kaufmann, "Digital coherent receiver based transmitter penalty characterization," *Optics Express*, vol. 24, no. 26, pp. 29 734–29 748, 2016.

[29] E. Benavent and A. Martínez, "Multi-depot multiple TSP: A polyhedral study and computational results," *Annals of Operations Research*, vol. 207, no. 1, pp. 7–25, 2013.

[30] P. Poggiolini and Y. Jiang, "Recent advances in the modeling of the impact of nonlinear fiber propagation effects on uncompensated coherent transmission Systems," *Journal of Lightwave Technology*, vol. 35, no. 3, pp. 458–480, 2017.

[31] B. Chandra, H. Karloff, and C. Tovey, "New results on the old k-opt algorithm for the traveling salesman problem," *SIAM Journal on Computing*, vol. 28, no. 6, pp. 1998–2029, 1999.

[32] B. C. Chatterjee, N. Sarma, and E. Oki, "Routing and spectrum allocation in elastic optical networks: a tutorial," *IEEE Communications Surveys and Tutorials*, vol. 17, no. 3, pp. 1776–1800, 2015.